

## Antitumor Activity and DNA-Binding Investigations of the Zn(II) and Cu(II) Complexes with Isoeuxanthone

Huifang WANG,<sup>a</sup> Rui SHEN,<sup>b</sup> Jincai WU,<sup>a</sup> and Ning TANG\*<sup>a</sup>

<sup>a</sup> College of Chemistry and Chemical Engineering, State Key Laboratory of Applied Organic Chemistry, Lanzhou University; Lanzhou 730000, P. R. China; and <sup>b</sup> College of Pharmacy Nankai University; Tianjin 300071, P. R. China.

Received March 10, 2009; accepted May 12, 2009; published online May 15, 2009

Two new complexes ZnL<sub>2</sub> (1) and CuL<sub>2</sub> (2) (here, HL=isoeuxanthone) have been synthesized and characterized by elemental analyses, molar conductance, infrared spectra (IR), <sup>1</sup>H-NMR and UV-Vis measurements. The interactions of them with calf thymus DNA (ct DNA) have been investigated by absorption spectroscopy, fluorescence spectroscopy, circular dichroism spectroscopy and viscosity measurements. Experimental results revealed an intercalative interaction with DNA for the complexes; furthermore the binding affinity of 2 is higher than that of 1 according to the calculated binding constant values. In addition, they were evaluated for their cytotoxic activities toward human esophageal cancer (ECA109) and human gastric cancer (SGC7901) cells by MTT assay. Both of them showed significant cytotoxic potency.

**Key words** isoeuxanthone; Zn(II) complex; Cu(II) complex; DNA-binding; intercalative mode; antitumor activity

Recently, more and more attention has been paid to xanthenes that are widely present as a class of secondary metabolites in some higher plants and microorganisms.<sup>1–3)</sup> These naturally occurring compounds and their synthetic analogs have been reported to exhibit multiple important pharmacological properties, such as anti-oxidant, anti-inflammatory, anti-malarial and anti-cancer activity, *etc.*<sup>4–9)</sup> As shown in Fig. 1a, xanthenes having three linear fused aromatic rings may be viewed as flavone derivatives in which the phenyl group is fused with the two aromatic rings. This structural ‘similarity,’ together with the aforementioned studies on hydroxyflavones and biological efficacy of xanthenes enforced many scientists to isolate or synthesize appropriately modified derivatives for the development of prospective new drug candidates.<sup>10–12)</sup> Isoeuxanthone (Fig. 1b) is one of well-known xanthone derivatives which have diverse biological profiles.

Since DNA is an important cellular receptor, many chemicals exert their antitumor effects to DNA thereby changing the replication of DNA and inhibiting the growth of the tumor cell, which is the basis of designing new and more efficient anticancer drugs and their effectiveness depends on the mode and affinity of the binding.<sup>13)</sup> Similarly, interactions of metallic antitumor reagents with DNA are also very important in understanding the mechanisms of their antitumor activities.<sup>14,15)</sup> We were thus motivated to investigate metallic complexes of isoeuxanthone on their binding modes and affinities to DNA. Therefore, in this context, we report the synthesis and characterization of the mononuclear Zn(II) complex (1) and Cu(II) complex (2) with isoeuxanthone. The interactions of them with calf thymus (ct DNA) have also been studied by absorption spectroscopy, fluorescence spectroscopy, circular dichroism spectroscopy and viscosity

measurements. In addition, they were evaluated for their cytotoxic activities toward human esophageal cancer (ECA109) and human gastric cancer (SGC7901) cells by microculture tetrazolium (MTT) method.

### Experimental

**Materials** The ligand HL (isoeuxanthone, namely 1,6-dihydroxyxanthone) was prepared according to the literature<sup>16)</sup> with some improvement. All the chemicals were reagent grade and were used without further purification. Calf thymus DNA (ct DNA) and ethidium bromide (EB) were obtained from Sigma Chemical Co. All the measurements involving the interactions of the two complexes with ct DNA were carried out in doubly distilled water buffer containing 5 mM Tris[Tris(hydroxymethyl)-aminomethane] and 50 mM NaCl, and adjusted to pH 7.1 with hydrochloric acid. UV-Vis spectrometer was employed to check a solution of ct DNA purity ( $A_{260}:A_{280}>1.80$ ) and the concentration ( $\epsilon=6600\text{ M}^{-1}\text{ cm}^{-1}$  at 260 nm) in the buffer.<sup>17,18)</sup>

**Physical Measurements** Elemental analyses were conducted using an Elementar Vario EL elemental analyzer. The metal contents of the complexes were determined by titration with EDTA (ethylenediamine tetraacetic acid). Infrared spectra (4000–400 cm<sup>-1</sup>) were performed on a satellite FTIR spectrometer (Thermo Mattson) with KBr as discs. Mass spectrometry was obtained on Esquire6000 mass spectrometer (Bruker Daltonics). <sup>1</sup>H-NMR spectra were recorded using a Varian Mercury Plus 400 spectrometer. Conductivity measurements were performed in *N,N*-dimethylformamide (DMF) with a DDS-11A conductor at room temperature. The UV-Vis absorption spectra were recorded using a Varian Cary 100 spectrophotometer and fluorescence emission spectra were recorded using a Hitachi F-4500 spectrofluorophotometer. The circular dichroism (CD) spectra were recorded on a Jasco J-810 spectropolarimeter.

**Methods** Absorption titration experiments were performed by fixing concentration of the two complexes as constant at 10 μM while varying the concentrations of ct DNA. The competitive binding experiments were carried out by maintaining the EB and ct DNA concentration at 3 μM and 30 μM, respectively, while increasing the concentrations of the complexes. Fitting was completed using an Origin 6.0 spreadsheet, where values of the binding constants  $K_b$  were calculated.

The CD spectra of DNA were recorded on a Jasco J-810 spectropolarimeter at 25.0±0.1 °C. Calf thymus DNA used were 100 μM in concentration and complexes solutions were added to a ratio of 2 : 1 (DNA/complex). Each sample solution was scanned in the range of 220–450 nm. CD spectrum was generated which represented the average of three scans from which the buffer background had been subtracted.

Viscosity experiments were carried out on an Ubbelohde viscometer, immersed in a thermostated water-bath maintained to 25.0±0.1 °C. Titrations were performed for the complexes (1–6 μM), and each sample was introduced into DNA solution (50 μM) present in the viscometer. Flow time was measured with a digital stopwatch and each sample was measured three

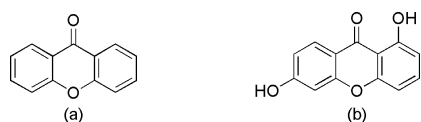


Fig. 1. Structure of Xanthone (a) and Isoeuxanthone (b)

\* To whom correspondence should be addressed. e-mail: tangn@lzu.edu.cn

times, then an average flow time was calculated. Data were presented as  $(\eta/\eta_0)^{1/3}$  versus the ratio of the concentration of the complex and DNA, where  $\eta$  is the viscosity of DNA in the presence of complex, and  $\eta_0$  is the viscosity of DNA alone. Viscosity values were calculated from the observed flow time of DNA-containing solution corrected from the flow time of buffer alone ( $t_0$ ),  $\eta = t - t_0$ .<sup>19,20</sup>

**Preparation of the Complexes** The complex **1** was prepared as follows. The ligand (**HL**) (91.6 mg, 0.4 mmol) was dissolved in 5 ml of ethanol at 90 °C, and then solid NaOH (16 mg, 0.4 mmol) was added. After 0.5 h, Zn(OAc)<sub>2</sub>·2H<sub>2</sub>O (43.9 mg, 0.2 mmol) was dissolved in 2 ml of ethanol and added dropwise to the above solution. The mixture was stirred for 8 h at room temperature. Then yellow precipitated residue was obtained after being washed several times with ethanol and centrifuged. Yellow solid was afforded and dried *in vacuo* for 48 h. Yield: 55.3 mg (49.8%). <sup>1</sup>H-NMR (400 MHz, DMSO-*d*<sub>6</sub>, 25 °C)  $\delta$  (ppm): 7.95–7.92 (1H, t), 7.63–7.59 (1H, t), 7.15–7.13 (2H, d), 6.73–6.71 (2H, d). IR  $\nu_{\max}$  (cm<sup>-1</sup>):  $\nu$  (–OH): 3401,  $\nu$  (C=O): 1603,  $\nu$  (C=C): 1450,  $\nu$  (Ar–O): 1228,  $\nu$  (C–O–C): 1170,  $\nu$  (Ar–H): 916/721,  $\nu$  (M–O): 486. MS  $m/z$ : 518.7 [M+H]<sup>+</sup>. Elemental Anal. Calcd for C<sub>26</sub>H<sub>14</sub>O<sub>8</sub>Zn: C, 60.08; H, 2.71; Zn, 12.58%. Found: C, 59.96; H, 2.75; Zn, 12.50%.  $A_M$  (S cm<sup>2</sup> mol<sup>-1</sup>): 8.4.

The synthesis of the complex **2** is identical to that of **1**. A yellow-green solid was collected. Yield: 72.3 mg (65.3%). IR  $\nu_{\max}$  (cm<sup>-1</sup>):  $\nu$  (–OH): 3398,  $\nu$  (C=O): 1608,  $\nu$  (C=C): 1472,  $\nu$  (Ar–O): 1234,  $\nu$  (C–O–C): 1178,  $\nu$  (Ar–H): 921/703,  $\nu$  (M–O): 487 cm<sup>-1</sup>. MS  $m/z$ : 517.8 [M+H]<sup>+</sup>. Elemental Anal. Calcd for C<sub>26</sub>H<sub>14</sub>O<sub>8</sub>Cu: C, 60.29; H, 2.72; Cu, 12.27%. Found: C, 60.17; H, 2.69; Cu, 12.32%.  $A_M$  (S cm<sup>2</sup> mol<sup>-1</sup>): 24.7.

**Antitumor Activity Assay** Two different human cancer cell lines, human esophageal cancer cell (ECA109) and human gastric cancer cell (SGC7901), were purchased from Shanghai Institutes for Biological Sciences, Chinese Academy of Sciences. They were cultured on RPMI-1640 medium supplemented with fetal bovine serum (10%), penicillin (100 U/ml) and streptomycin (100  $\mu$ g/ml) in 25 cm<sup>2</sup> culture flasks at 37 °C in a humidified atmosphere with 5% CO<sub>2</sub>.

For the drug treatment experiments, the cancer cells were harvested from the culture during the exponential growth phase, and seeded into multiwell culture plates at 5 × 10<sup>4</sup> cells/ml in fresh medium. Following 24 h incubation at 37 °C, cells were treated for 72 h to six grade concentrations in triplicate of the test drug. At the end of the drug treatment period, 10  $\mu$ l of MTT solution (5 mg/ml) was added directly to all the appropriate wells and then the culture was incubated for 4 h. Thereafter the formazan crystal formed in the well was solubilized with DMSO and 100  $\mu$ l of SDS (10%) was added to the system. After the plates were incubated overnight, the optical density was read on microplate spectrophotometer at 570 nm. Results are expressed as IC<sub>50</sub> (mean,  $n=3$ ), which is defined as the drug concentration inhibiting the absorbance by 50% with respect to that of untreated cells.

## Results and Discussion

**Characterization of the Complexes** The two complexes are air stable for extended periods and soluble in DMF and DMSO; slightly soluble in methanol, ethanol and acetone; insoluble in benzene and diethyl ether. The molar conductance values in DMF are 8.37 and 24.71 S cm<sup>2</sup> mol<sup>-1</sup> for **1** and **2**, respectively, which suggest that the two complexes are non-electrolyte.<sup>21</sup> The elemental analyses, molar conductivities, IR spectra, <sup>1</sup>H-NMR and UV-Vis measurements show that the formulas of the complexes conform to ML<sub>2</sub> [where M=Zn(II) and Cu(II)].

**IR Spectra** In the IR spectrum of the ligand,<sup>16</sup> valence carbonyl group vibrations  $\nu$  (C=O) coupled with the double band in the  $\gamma$ -benzopyrone ring appears at 1639 cm<sup>-1</sup>. However the bands of  $\nu$  (C=O) in **1** and **2** shift to 1603 and 1608 cm<sup>-1</sup>, respectively,  $\Delta\nu$  (ligand-complex) are 36 and 31 cm<sup>-1</sup>. These shifts demonstrate that group loses its original characteristics and forms a coordinative bond with Zn(II) ion or Cu(II) ion. The absorption bands at 3327 cm<sup>-1</sup> attributed to  $\nu$  (O–H) in the ligand shift to 3401 cm<sup>-1</sup> and 3398 cm<sup>-1</sup> for **1** and **2**, respectively; The weak bands at 486 cm<sup>-1</sup> and 487 cm<sup>-1</sup> are assigned to  $\nu$  (M–O),<sup>22</sup> suggest-

ing coordination of –OH with the Zn(II) ion or Cu(II) ion after deprotonation.

**<sup>1</sup>H-NMR Spectra** <sup>1</sup>H-NMR spectra of **1** was studied using DMSO-*d*<sub>6</sub> as solvent. Compared with <sup>1</sup>H-NMR of the ligand, the single peak ( $\delta$  12.82 ppm) due to the hydroxy proton (1-OH) of the free ligand disappeared. The change indicated that the oxygen of the deprotonated hydroxy group in the ligand coordinates to the Zn(II) ion. In addition, the shifts of the hydrogen in the phenyl were changed as a result of the coordination.

**Stoichiometry Study** UV-Vis measurements can be used in spectrophotometric titration to study equilibria and discuss the structures of complexes in aqueous solution.<sup>23</sup> Varying both the added concentration of Zn<sup>2+</sup> ( $C_{Zn}$ ) and the ligand ( $C_L$ ), the complex formation between them was investigated. Insight into the preferred stoichiometry was provided by an experiment in which the total concentration of Zn<sup>2+</sup> and ligand (**L**) was held fixed ( $C_{Zn} + C_L = 1.0 \times 10^{-5}$  M), varying the ratio of the components ( $C_{Zn}/C_L$ ). This was achieved by mixing equimolar solutions (1.0 × 10<sup>-5</sup> M) of the components. At about  $C_{Zn}/C_L = 1/2$ , the absorption intensity (at about 358 nm) was maximized, which is shown in Fig. 2a. Evidently, under these conditions 1:2 complex was formed, in other words, the Zn<sup>2+</sup> ion bound to two ligands.<sup>24</sup> The stoichiometric ratio of the Cu<sup>2+</sup> ion and the ligand in the complex **2** was determined by the similar way, which was identical to that of complex **1**, as shown in Fig. 2b.

Based on the results of elemental analyses, molar conductivities, IR spectra, <sup>1</sup>H-NMR and stoichiometry study, we speculated that the two ligands both acted as a bidentate ligand and formed mononuclear complex with Zn(II) ion or

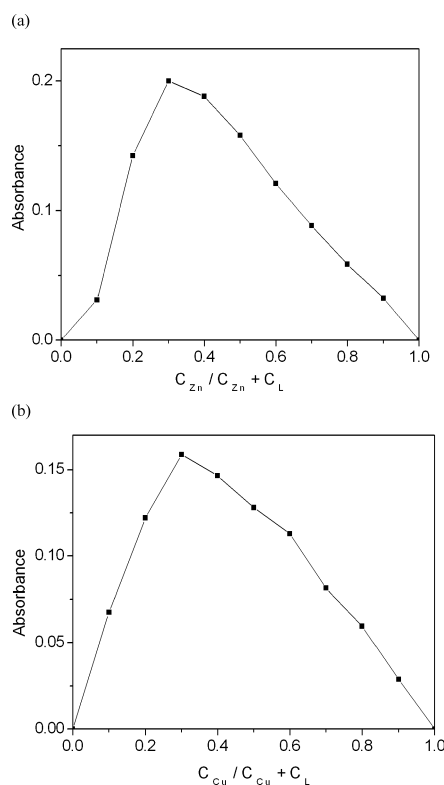


Fig. 2. Plot of the Complex Formation of Zn<sup>2+</sup> (a) and Cu<sup>2+</sup> (b) with Ligand (**L**), Monitored with a UV-Vis Spectrophotometer

$C_M + C_L = 1.0 \times 10^{-5}$  M was held in aqueous solution (M=Zn<sup>2+</sup>, Cu<sup>2+</sup>).

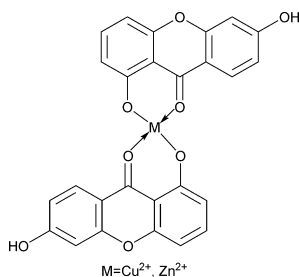


Fig. 3. Speculate Structure of the Complexes

Cu(II) ion. The likely structures of the complexes are shown in Fig. 3.

#### DNA-Binding Studies. Electronic Absorption Titration

Electronic absorption spectroscopy is universally employed to examine the binding mode of DNA with complexes.<sup>25)</sup> The absorption spectra of **1** and **2** in the absence and presence of ct DNA are given in Figs. 4a and b. In the absence of ct DNA, the UV-Vis absorption spectra of **1** has a strong  $\pi$ - $\pi^*$  transition band at  $\lambda_{\max}=227$  nm and a weak  $n$ - $\pi^*$  transition band at  $\lambda_{\max}=359$  nm, while the complex **2** has a strong  $\pi$ - $\pi^*$  transition band at  $\lambda_{\max}=241$  nm and a weak  $n$ - $\pi^*$  transition band at  $\lambda_{\max}=358$  nm. With increasing DNA concentration, the absorption bands of the two complexes show decreases in molar absorptivity (hypochromism) as well as slight bathochromism. These variations are strongly indicative of the intercalation mode of the two complexes with ct DNA, involving a strong  $\pi$ -stacking interaction between the compounds and DNA base pairs.

In order to study the binding ability of the complexes with DNA quantitatively, the binding constant  $K_b$  was determined using the Eq. 1,<sup>26)</sup>

$$[\text{DNA}]/(\varepsilon_a - \varepsilon_f) = [\text{DNA}]/(\varepsilon_b - \varepsilon_f) + 1/K_b(\varepsilon_b - \varepsilon_f) \quad (1)$$

where [DNA] is the concentration of ct DNA in base pairs,  $\varepsilon_a$ ,  $\varepsilon_f$ , and  $\varepsilon_b$  are the apparent extinction coefficient correspond to  $A_{\text{obsd}}/[M]$ , the extinction coefficient for the free compound and the extinction coefficient for the compound in the fully bound form, respectively. In plots of  $[\text{DNA}]/(\varepsilon_a - \varepsilon_f)$  versus [DNA],  $K_b$  is given by the ratio of slope to the intercept (Figs. 4a, b, inset). The binding constants  $K_b$  for **1** and **2** were found to be  $1.8 \times 10^4 \text{ M}^{-1}$  and  $2.5 \times 10^4 \text{ M}^{-1}$ , respectively. The results indicate that the binding strength of the complex **2** is stronger than **1**.

**Fluorescence Spectra** Further support for the complexes binding to DNA by intercalation mode was given through the competitive binding experiment. EB is a conjugate planar molecule. Its fluorescence intensity is very weak, but the intensity greatly increases when EB intercalated into DNA. When a second ligand is added, it could compete with EB for DNA binding sites and then a decrease in the fluorescence intensity is observed. Therefore EB can be used as a common fluorescent probe for DNA structure and has been employed in investigations of the mode and the process of metal complex binding to DNA.<sup>27,28)</sup>

The emission spectra of DNA-EB system in the presence of increasing amounts of **1** and **2** are shown in Figs. 5a and b. The emission intensity of DNA-EB system at 587 nm decreased apparently when the concentration of the complexes increased and an isoactinic point appeared at about 535 nm,

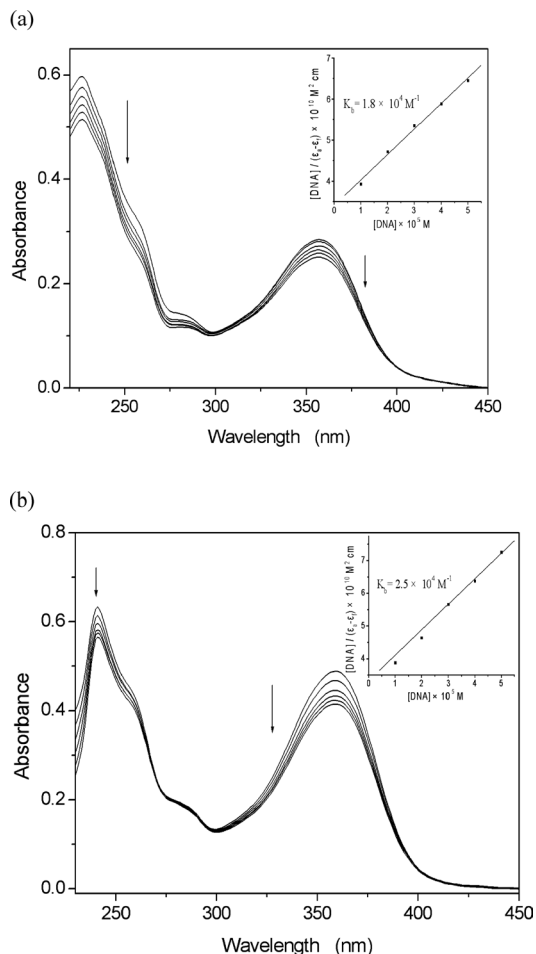


Fig. 4. UV-Vis Absorption Spectra of **1** (a) and **2** (b) ( $10 \mu\text{M}$ ) in the Presence of Increasing Amounts of ct DNA

[DNA]=0, 10, 20, 30, 40, 50  $\mu\text{M}$ . The arrow indicates the absorbance changes upon increasing DNA concentration. The inset is plot of  $[\text{DNA}]/(\varepsilon_a - \varepsilon_f)$  vs. [DNA] for the titration of DNA to complex.

which confirms that both complexes interact with DNA by an intercalating mechanism, competing with EB for the same binding sites.<sup>29)</sup>

According to the classical Stern-Volmer Eq. 2<sup>30)</sup>:

$$F_0/F = 1 + K_q[Q] \quad (2)$$

Where  $F_0$  and  $F$  represent the emission intensity in the absence and presence of quencher, respectively,  $K_q$  is a linear Stern-Volmer quenching constant and  $[Q]$  is the quencher concentration. The quenching plots illustrate that the quenching of EB bound to DNA by the complexes is in good agreement with the linear Stern-Volmer equation (Figs. 5a, b, inset). In the plots of  $F_0/F$  versus  $[Q]$ ,  $K_q$  is given by the ratio of the slope to the intercept. The  $K_q$  value for the complex **1** is  $1.2 \times 10^4 \text{ M}^{-1}$  while the  $K_q$  value for the complex **2** is  $2.2 \times 10^4 \text{ M}^{-1}$ , which shows that **2** is more able than **1** in replacing the strong DNA intercalator EB. This result suggests that the binding affinity of **2** is higher than **1**, being accordance with above absorption titration results.

**CD Spectroscopy** Circular dichroic spectral techniques may give us useful information on how the conformation of the DNA chain is influenced by the bound complex. The CD spectrum of ct DNA consists of a positive band at 275 nm that can be due to base stacking and a negative band at

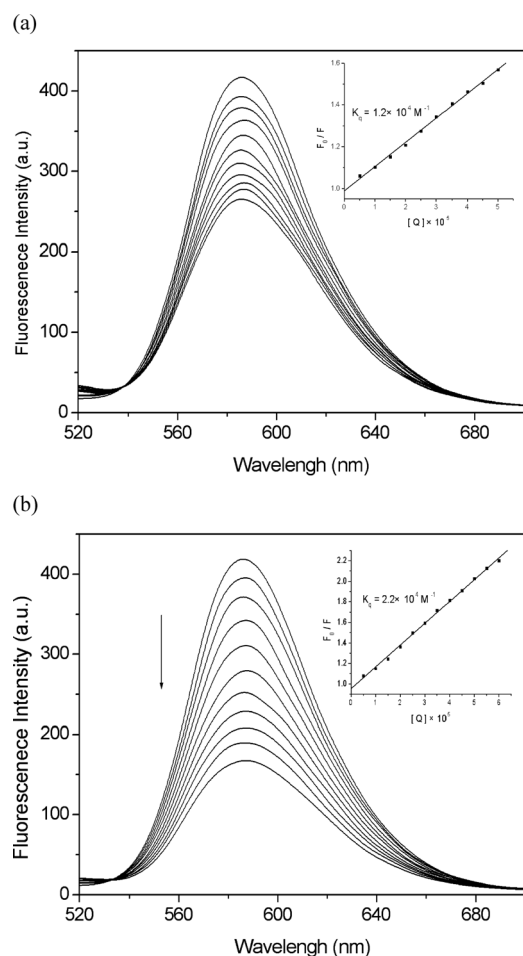


Fig. 5. Fluorescence Emission Spectra of DNA-EB in the Presence of 0, 5, 10, 15, 20, 25, 30, 35, 40, 45, 50  $\mu\text{M}$  of **1** (a) and **2** (b)

$\lambda_{\text{em}} = 500 \text{ nm}$ ,  $\lambda_{\text{exc}} = 520\text{--}700 \text{ nm}$ .  $[\text{EB}] = 3 \mu\text{M}$ ,  $[\text{DNA}] = 30 \mu\text{M}$ . The inset is Stern-Volmer quenching plots of the fluorescence titration.

245 nm that can be due to helicity and it is also characteristic of DNA in a right-handed B form.<sup>31)</sup> The changes in CD signals of DNA observed on interaction with drugs may often be assigned to the corresponding changes in DNA structure.<sup>32)</sup> Thus simple groove binding and electrostatic interaction of small molecules show less or no perturbation on the base-stacking and helicity bands, whereas intercalation enhances the intensities of both the bands stabilizing the right-handed B conformation of ct DNA as observed for the classical intercalators.<sup>33)</sup>

The CD spectrum of ct DNA was monitored in the presence of **1** and **2**; the changes observed in the two cases are shown in Fig. 6. The complexes show spectral changes, high increase in intensity of both the positive and negative bands, which are typical of strong intercalation involving  $\pi$ -stacking and stabilization of the right-handed B form of ct DNA. Further, the increase in intensity observed for the complex **2** is higher than the complex **1**, which is in agreement with the DNA binding constants. Thus the CD spectral results certify the intercalative mode of DNA binding for the present complexes furtherly. It is possible that the extended aromatic rings reduce the helical twist angle of the DNA base pairs and increase the intensity of the base stacking band.<sup>33)</sup>

**Viscosity Studies** Optical photophysical probes generally provide necessary, but not sufficient clues to support a

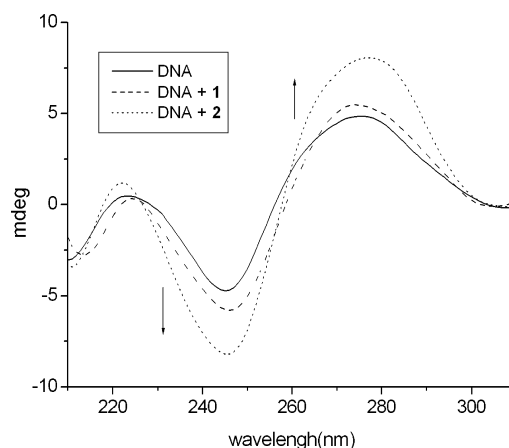


Fig. 6. CD Spectra of ct DNA ( $100 \mu\text{M}$ ) in the Absence and Presence of **1** ( $50 \mu\text{M}$ ) and **2** ( $50 \mu\text{M}$ )

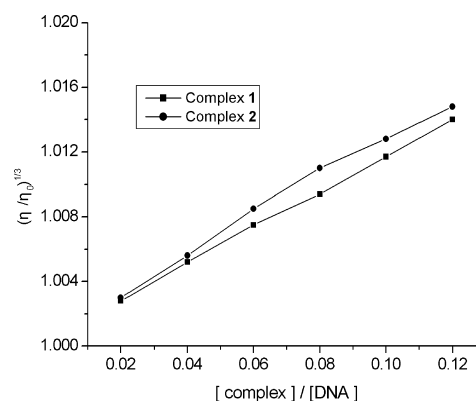


Fig. 7. Effect of Increasing Amounts of the Complex **1** and **2** on the Relative Viscosity of ct DNA at  $25 \text{ }^\circ\text{C}$

$[\text{DNA}] = 50 \mu\text{M}$ ,  $[\text{complex}] = 1, 2, 3, 4, 5, 6 \mu\text{M}$ .

binding model. Hydrodynamic measurements that are sensitive to length change (*i.e.*, viscosity and sedimentation) are regarded as the least ambiguous and the most critical tests of binding in solution in the absence of crystallographic structural data. A classical intercalation model results in lengthening the DNA helix as base pairs are separated to accommodate the binding small molecules, leading to an increase of DNA viscosity. In contrast, a partial and non-classical intercalation of small molecules could bend or kink the DNA helix, reduce its effective length and, concomitantly, its viscosity.<sup>34)</sup>

As a validation of the above verdict, viscosity measurements were carried out. The effects of the two complexes on the viscosity of DNA at  $25.0 \pm 0.1 \text{ }^\circ\text{C}$  are shown in Fig. 7. It can be observed that the viscosity of the DNA increase steadily with increasing amounts of **1** and **2**. Such behavior is in accordance with other intercalators, which increases the relative specific viscosity for the lengthening of the DNA double helix resulting from intercalation. These results indicate that the two complexes can intercalate between adjacent DNA base pairs, causing an extension in the helix, and thus increase the viscosity of DNA. **2** can intercalate more deeply than that of **1**. The results obtained from viscosity studies also validate those obtained from the spectroscopic studies. On the basis of all the spectroscopic studies together with the

Table 1. Cytotoxic Activity *in Vitro* of the Complexes

Complex	Cytotoxic activities IC <sub>50</sub> (μg/ml)	
	ECA109	SGC7901
<b>1</b>	30.7	33.2
<b>2</b>	20.8	25.7

viscosity measurements, it is suggested that the two complexes can bind to ct DNA in intercalative mode.

**Antitumor Activity** Evaluation of the two complexes for cytotoxic activity *in vitro* was performed by MTT assay using two different human cancer cell lines, human esophageal cancer cell (ECA109) and human gastric cancer cell (SGC7901). The cultured cell lines were divided into multi-well microplate and treated with the synthesized compounds. The resulting solutions were detected and evaluated for their biological activities.

The assessments of cytotoxic activities were expressed as the concentration inhibiting 50% of cancer cell growth (IC<sub>50</sub>). The results were summarized in Table 1, which showed that **2** had more significant cytotoxic activities than **1** against the human cancer cell lines. The result of inhibitory effect *in vitro* is consistent with the result of DNA binding studies above, which may be due to the complexes inducing DNA damage in cancer cells<sup>35</sup> and the nature of the metal ions.<sup>36,37</sup>

## Conclusion

The two new complexes ZnL<sub>2</sub> (**1**) and CuL<sub>2</sub> (**2**) (here, HL=1,6-dihydroxyxanthone) have been successfully synthesized. The DNA binding properties of complexes have been studied by spectrophotometric methods and viscosity measurements. The results suggest that the complexes intercalate into the base group pairs of DNA because of the good planarity of the xanthone ring. They both have strong binding affinity with DNA. Comparing the binding constants of them, it is concluded that binding affinity of the complex **2** is stronger than that of the complex **1**. Furthermore, assay *in vitro* of them showed a remarkable antitumor activity towards ECA109 and SGC7901 cell lines. Information obtained from the present work may be helpful to the research of the action mechanism of metallic anticancer reagents.

**Acknowledgment** We are grateful for the financial support of the National Science Foundation of China (20601011).

## References

- Pinto M. M. M., Sousa M. E., Nascimento M. S., *J. Curr. Med. Chem.*, **12**, 2517—2538 (2005).
- Peres V., Nagem T. J., Oliveira F. F. D., *Phytochemistry*, **55**, 683—710 (2000).
- Jung H. A., Su B. N., Keller W. J., Mehta R. G., Kinghorn A. D., *J. Agric. Food Chem.*, **54**, 2077—2082 (2006).
- Lee B. W., Lee J. H., Lee S. T., Lee H. S., Lee W. S., Jeong T. S., Park K. H., *Bioorg. Med. Chem. Lett.*, **15**, 5548—5552 (2005).
- Lin C. N., Chung M. I., Liou S. J., Lee T. H., Wang J. P., *J. Pharm. Pharmacol.*, **48**, 532—538 (1996).
- Pedro M., Cerqueira F., Sousa M. E., Nascimento M. S. J., Pinto M., *Bioorg. Med. Chem.*, **10**, 3725—3730 (2002).
- Valenti P., Bisi A., Rampa A., Belluti F., Gobbi S., Zampiron A., Carrara M., *Bioorg. Med. Chem.*, **8**, 239—246 (2002).
- Yoshimi N., Matsunaga K., Katayama M., Yamada Y., Kuno T., Qiao Z., Hara A., Yamahara J., Mori H., Naoki Y., *Cancer Lett.*, **163**, 163—170 (2001).
- Sanugul K., Akao T., Li Y., Kakiuchi N., Nakamura N., Hattori M., *Biol. Pharm. Bull.*, **28**, 1672—1678 (2005).
- Truscheit E., Frommer W., Junge B., Muller L., Schmidt D. D., Wingender W., *Angew. Chem. Int. Ed. Engl.*, **20**, 744—761 (1981).
- McCulloch D. K., Kurtz A. B., Tattersall R. B., *Diabetes Care*, **6**, 483—487 (1983).
- Sou S., Takahashi H., Yamasaki R., Kagechika H., Endo Y., Hashimoto Y., *Chem. Pharm. Bull.*, **49**, 791—793 (2001).
- Pyle A. M., Morii T., Barton J. K., *J. Am. Chem. Soc.*, **112**, 9432—9434 (1990).
- Satyanarayana S., Dabrowiak J. C., Chaires J. B., *Biochemistry*, **31**, 9319—9324 (1992).
- Hiort C., Lincoln P., Norden B., *J. Am. Chem. Soc.*, **115**, 3448—3454 (1993).
- Liu Y., Zou L., Ma L., Chen W. H., Wang B., Xu Z. L., *Bioorg. Med. Chem.*, **14**, 5683—5690 (2006).
- Huang C. Z., Li Y. F., Feng P., *Talanta*, **55**, 321—328 (2001).
- Kumar C. V., Asuncion E. H., *J. Am. Chem. Soc.*, **115**, 8547—8553 (1993).
- Eriksson M., Leijon M., Hiort C., Norden B., Graslund A., *Biochemistry*, **33**, 5031—5040 (1994).
- Xiong Y., He X. F., Zou X. H., Wu J. Z., Chen X. M., Ji L. N., Li R. H., Zhou J. Y., Yu K. B., *J. Chem. Soc. Dalton Trans.*, **1999**, 19—24 (1999).
- Geary W. J., *Coord. Chem. Rev.*, **7**, 81—122 (1971).
- Nakamoto K., "Infrared and Raman Spectra of Inorganic and Coordination Compounds," 4th ed., Wiley & Sons, 1986, p. 266.
- Peters M., Siegfried L., Kaden T. A., *J. Chem. Soc. Dalton Trans.*, **2000**, 4664—4668 (2000).
- Werth M. H. V., Verhoeven J. W., Hofstraat J. W., *J. Chem. Soc. Perkin Trans.*, **2**, **2000**, 433—439 (2000).
- Kelly J. M., Murphy M. J., Mcconnell D. J., Ohuigin C., *Nucleic Acids Res.*, **13**, 167—184 (1985).
- Mudasir, Yoshioka N., Inoue H., *J. Inorg. Biochem.*, **77**, 239—247 (1999).
- Lippard S. J., *Acc. Chem. Res.*, **11**, 211—217 (1978).
- Lepecq J. B., Paoletti C., *J. Mol. Biol.*, **27**, 87—106 (1967).
- Zeng Y. B., Yang N., Liu W. S., Tang N., *J. Inorg. Biochem.*, **97**, 258—264 (2003).
- Efink M. R., Ghiron C. A., *Anal. Biochem.*, **114**, 199—227 (1981).
- Ivanov V. I., Minchenkova L. E., Schyolkina A. K., Poletayer A. I., *Biopolymers*, **12**, 89—110 (1973).
- Lincoln P., Tuite E., Norden B., *J. Am. Chem. Soc.*, **119**, 1454—1455 (1997).
- Norden B., Tjerneld F., *Biopolymers*, **21**, 1713—1734 (1982).
- Zou X. H., Ye B. H., Li H., Liu J. G., Xiong Y., Ji L. N., *J. Chem. Soc. Dalton Trans.*, **1999**, 1423—1428 (1999).
- Zuber G., Quada J. C. J., Hecht S. M., *J. Am. Chem. Soc.*, **120**, 9368—9369 (1998).
- Viola-Rhenals M., Rieber M. S., Rieber M., *Biochem. Pharmacol.*, **71**, 722—734 (2006).
- Daniela K. G., Gupta P., Harbach R. H., Guida W. C., Dou Q. P., *Biochem. Pharmacol.*, **67**, 1139—1151 (2004).